Potential model for the elastic scattering of electrons by helium at intermediate energies

Joseph M. Paikeday

Southeast Missouri State University, Cape Girardeau, Missouri 63701
(Received 13 February 1976)

Differential scattering cross section of electrons scattered elastically by helium atoms is computed using a model potential constructed from the Hartree–Fock wavefunction of Roothan, Sachs, and Weiss and a three parameter phenomenological potential to account for the effects of long range polarization effects and nonlocal dynamic effects. The results are in good agreement with the recently published experimental data of Bromberg. The calculated values of the partial wave phase shifts agree with those of Ganas, Dutta, and Green and LaBahn and Callaway for angular momentum in the range $0 < l < 10$ within 5%. Results indicate that the model based on the Hartree–Fock wavefunction and a three parameter polarization potential can predict the scattering cross section at intermediate energies within a few percent of the experimental data. On the basis of the computed cross sections in 200–700 eV range, the approximate effective electron helium interaction potential for the quantum mechanical scattering problem is found to be $V_e(r) \simeq <\Phi_0|V(\mathbf{r},\mathbf{r}_1,\mathbf{r}_2)|\Phi_0> -(0.25+0.31r)\ e^{-2.8r} - \alpha_d(1+e^{-8r})[r^4+(1.3+E/350)^4]^{-1}$. The forward scattering amplitudes calculated from this model and corrected for electron exchange scattering compare favorably with the results of dispersion relation and eikonal optical model theories.

I. INTRODUCTION

The elastic scattering of an electron by an atom has been a subject of considerable theoretical and experimental interest.[1] For electron–helium problems, various approximation methods have been applied, among which are some of the well-known techniques such as the close-coupling[2] method, variational techniques,[3] and the polarized orbital method.[4] The first method involves the solution of a set of coupled differential equations to obtain the R and S matrices.[5] This is achieved by numerical solution provided a limited number of channels are included. This method is applicable at sufficiently low or at high enough energies so that only a few channels take part in the scattering problem.[6] This, however, is not suitable at intermediate energies. Variational techniques are somewhat general in that the problem is associated with the evaluation and minimization of lengthy integrals containing large number of variational parameters. The polarized orbital method originally proposed by Temkin and Lamkin[7] has been applied to the electron–helium problem by LaBahn and Callaway.[8] Their method involves the solution of the appropriate integrodifferential equation using the numerical methods and the computation of a large number of partial wave phase shifts.[9] Among the various calculations reported, only very few have been along the lines of the optical potential method. Mittleman[10] has incorporated the optical potential method to compute the electron–helium cross section in the intermediate range. A method of deriving the optical potential has been reported by Mittleman and Watson.[11] A somewhat different approach to the optical potential method is to select an appropriate form of the potential function with few parameters, which are then determined from a theoretical and experimental basis. Ganas, Dutta, and Green[12] have computed the cross section from this point of view and their results are in good agreement with the experimental data of Bromberg.[13] Since then, Bromberg[14] has reported revised cross section data in the energy range 200–700 eV which differ from the earlier results by a few percent in certain angular ranges. The purpose of the present work is to compute the scattering cross section using a somewhat more accurate model for the electron–helium interaction potential. In the present calculations, the static part is the same as the first order term of the optical potential, which is computed from the Hartree–Fock ground state wavefunction[15] and the dynamic part is approximated by a three parameter phenomenological potential. It is found that the cross section computed using the static and polarization potentials differ from the experimental data by 5% to 10% in the angular range $5° < \theta < 25°$ at intermediate energies. To account for this, a correction term is added to the potential, which is derived from a modified form of the target wavefunction. With this added correction to the potential, the calculated values agree with the data of Bromberg within 5% on an average for the range of scattering angles $1° < \theta < 40°$. The absolute differential scattering cross sections at the energies 100, 200, 300, 400, 500, and 700 eV have been computed in the range of scattering angles $1° < \theta < 30°$ for which the recent experimental data became available. For each incident energy of the electron, 200 partial wave phase shifts have been used. For the forward scattering amplitudes, up to 10 000 partial waves were needed. The potential function and its derivation is described in Sec. II. The details of the numerical method used for the computation of partial wave phase shifts are described in Sec. III and a discussion of the results and comparison with other calculations are presented in Sec. IV.

II. POTENTIAL MODEL FOR THE SCATTERING PROBLEM

The potential used in the present work consists of two parts: the static part and the dynamic part. For the static part, the potential is constructed from the ground state helium wavefunction, and for the dynamic part, a three parameter potential function of the Buckingham[16] type is selected on the basis that (a) it should

have the proper long range behavior of the polarization potential[17] for helium, (b) it should have the proper analytical properties for the convergence of the partial waves sum, and (c) the computed scattering amplitudes should agree with the experimental values at a selected scattering angle within a small, preassigned value. In the notation of Watson,[18] the optical potential is given by

$$V_{\mathrm{OPT}} = \langle \Phi_0 | V | \Phi_0 \rangle + \sum \frac{\langle \Phi_0 | V | \Phi_n \rangle \langle \Phi_n | V | \Phi_0 \rangle}{p^2 - T - W_n + W_0 + i\epsilon} + \text{higher order terms}, \quad (2.1)$$

where the first part is the static potential which is given in Eq. (2.9) and the second part contains excited states of the target atom. The direct computation of the second or higher order terms is not attempted here. Instead, all the missing terms is approximated by a phenomenological potential $V_p(r)$ so that the equivalent one particle problem given by

$$[\nabla^2 + k^2 + \langle 0 | V | 0 \rangle + V_p(r)]\Phi(r) = 0 \quad (2.2)$$

corresponds to the experimental value of the scattering cross section for a certain angle θ in the range $0° < \theta < 10°$. A first approximation to the potential $V_p(r)$ can be obtained by using the Born approximation since the energy range 200–700 eV is favorable. Thus, if one were to vary a parameter contained in $V_p(r)$, a reasonable starting value can be obtained from the Born approximation given by[19]

$$f^B(\theta) = -\frac{2m}{\hbar^2}\int \frac{\sin Kr}{Kr} V_e(r) r^2 dr . \quad (2.3)$$

It may be noted that if one were to obtain a potential $V_p^B(r)$ such that the $f^B(\theta)$ agrees with the experimental scattering amplitude, the scattering amplitude $f^S(\theta)$ obtained from Eq. (2.2) using the potential $V_p^B(r)$ will be different from the experimental scattering amplitude even at intermediate energies. From actual computations with various potential functions, it is found that the difference is more pronounced at small scattering angles in the range $0° < \theta < 10°$. Thus, the trial form of $V_p(r)$ is made to satisfy the equation

$$f^B(\theta) = -\frac{2m}{\hbar^2}\left[\int \frac{\sin Kr}{Kr} \langle 0 | V | 0 \rangle r^2 dr + \int V_p(r) \frac{\sin Kr}{Kr} r^2 dr\right] . \quad (2.4)$$

The long range form of $V_p(r)$ is generally known to have an assymptotic form of $\alpha_d r^{-4}$, where α_d is the dipole polarizability of the helium atom. The short range form of $V_p(r)$ depends on the dynamic part of the problem and is expected to be energy dependent. Thus, writing $V_p(r)$ in terms of the unknown function $g(r)$, one has $V_p(r) = \alpha_d r^{-4} g(r)$, where $\lim_{r\to 0} g(r) = 0$ and $\lim_{r\to\infty} \times g(r) = 1$ and the integral in the Born approximation, namely, $\int_0^\infty [\sin Kr\, g(r)/r^3]\, dr$ should converge. These conditions do not determine the function $g(r)$ uniquely, but somewhat restrict the nature of the function. To be able to evaluate the integral in the Born approximation, a cutoff parameter is needed so that $V_p(r)$ takes the form $\alpha_d g(r)/(r^4 + C)$ and a suitable form for $g(r)$ for the Born approximation is found to be an exponential type and thus $V_p(r)$ is selected and has the form

$$V_p(r) = -\alpha_d(1 - \gamma e^{-\delta r})(r^4 + C)^{-1} , \quad (2.5)$$

where the parameters C and δ are to be determined. To determine the values of δ and C within the Born approximation, a normalization condition is used, namely the computed scattering cross section at an angle θ_i agrees with the experimental data at the same angle. In the present work, θ_i is selected to be $= 2°$. In the IBM 370 computer it was found that for a fixed value of δ, the value of C that satisfies the above conditions within 2% can be found in a few minutes of computer time. When the function $V_p(r)$ obtained this way was substituted in Eq. (2.2), the scattering cross section at θ_i turned out to be greater than the experimental value by 10% to 30% depending on the energy. However, this presented no difficulty since a corrected set of parameters can be computed on the basis of an adjusted value for cross section data at θ_i. The adjustment of the data is based on the difference between the Schrödinger cross section and the Born cross section for a given potential $V_p(r)$. The recomputation of the parameters using the Born approximation is achieved in a few seconds of computer time since the numerical integration algorithm involves only a few hundred evaluations of the integrand. The details of the numerical method of computing the partial wave phase shifts is included in the next section.

A. The static potential

In Eq. (2.1) the first term consists of the nuclear and coulomb potentials and is given by (in atomic units)

$$\langle \Phi_0 | V | \Phi_0 \rangle = \langle \Phi_0 | \frac{2}{r} - \frac{1}{|\mathbf{r} - \mathbf{r}_1|} - \frac{1}{|\mathbf{r} - \mathbf{r}_2|} | \Phi_0 \rangle , \quad (2.6)$$

where $\mathbf{r}_1$ and $\mathbf{r}_2$ are the position vectors of the atomic electrons and $\mathbf{r}$ is the position vector of the incident electron relative to the helium nucleus. In Eq. (2.6), $\Phi_0(\mathbf{r}_1, \mathbf{r}_2)$ is the normalized ground state wavefunction of the helium atom constructed from the SCF orbitals of Roothan, Sachs, and Weiss[20] in the form

$$R_{\lambda\rho}(r) = [(2\eta_{\lambda\rho})!]^{-1/2}(2\xi_{\lambda\rho})^{\eta_{\lambda\rho}+1/2} r^{\eta_{\lambda\rho}-1} e^{-\xi_{\lambda\rho} r} . \quad (2.7)$$

For helium, this is given by

$$\Phi_{1s}(r) = \left[C_1 \frac{(2\xi_1)^{3/2}}{\sqrt{2!}} + C_2 \frac{(2\xi_1)^{5/2}}{\sqrt{4!}} r\right] e^{-\xi_1 r} + \left[C_3 \frac{(2\xi_2)^{3/2}}{\sqrt{2!}} + C_4 \frac{(2\xi_2)^{5/2}}{\sqrt{4!}} r\right] e^{-\xi_2 r} , \quad (2.8)$$

where the constants C_1, C_2, C_3, C_4, and ξ_1 and ξ_2 are given as $C_1 = 0.175261$, $C_2 = 0.010673$, $C_3 = 0.884315$, $C_4 = 0.051269$, $\xi_1 = 3$, and $\xi_2 = 1.4$. Using the orbital function defined in Eq. (2.8) in evaluating Eq. (2.6) the following expression for the static potential results (in Ry):

$$\langle\Phi_0|V|\Phi_0\rangle = -e^{-2\alpha r}\left[\frac{A^2}{\alpha^3}\left(\frac{1}{r}+\alpha\right)+\frac{AB}{2\alpha^4}\left(\frac{6}{r}+8\alpha+4\alpha^2 r\right)+\frac{B^2}{8\alpha^5}\left(\frac{24}{r}+36\alpha+24r\alpha^2+8r^2\alpha^3\right)\right]$$

$$-e^{-2\beta r}\left[\frac{C^2}{\beta^3}\left(\frac{1}{r}+\beta\right)+\frac{CD}{2\beta^4}\left(\frac{6}{r}+8\beta+4\beta^2 r\right)+\frac{D^2}{8\beta^5}\left(\frac{24}{r}+36\beta+24\beta^2 r+8\beta^3 r^2\right)\right]-e^{-(\alpha+\beta)r}\left\{\frac{16AC}{(\alpha+\beta)^3}\left(\frac{1}{r}+\frac{\alpha}{2}+\frac{\beta}{2}\right)\right.$$

$$\left.+\frac{8(BC+AD)}{(\alpha+\beta)^4}\left[\frac{6}{r}+4(\alpha+\beta)+r(\alpha+\beta)^2\right]+\frac{8BD}{(\alpha+\beta)^5}\left[\frac{24}{r}+18(\alpha+\beta)+6(\alpha+\beta)^2 r+(\alpha+\beta)^3 r^2\right]\right\}, \quad (2.9)$$

where the constants A, B, C, and D are obtained from C_1, C_2, C_3, and C_4 as $A=1.82136574$, $B=0.192114$, $C=2.9297397$, $D=-0.1372917$, $\alpha=3$, and $\beta=1.4$. The diamagnetic susceptibility of the atom using the equation[21]

$$\chi=\tfrac{1}{6}N\alpha_0^2 a_0^3\langle\Phi_0|r_1^2+r_2^2|\Phi_0\rangle \quad (2.10)$$

reduces to the expression given by

$$\chi=[1.5(A^2\alpha^{-5}+C^2\beta^{-5})+(45/4)(B^2\alpha^{-7}+D^2\beta^{-7})$$
$$+(15/2)(AB\alpha^{-6}+CD\beta^{-6})+96AC(\alpha+\beta)^{-5}$$
$$+480(BC+AD)(\alpha+\beta)^{-6}+2880\,BD(\alpha+\beta)^{-7}]\tfrac{1}{6}N\alpha_0^2 a_0^3. \quad (2.11)$$

Equation (2.11) gives a value of 1.862×10^{-6} e.m.u. $g^{-1}\cdot mole^{-1}$, which agrees with the experimental value of 1.88×10^{-6} e.m.u. $g^{-1}\cdot mole^{-1}$.

B. Correction to the static potential

With the potential defined by Eq. (2.9) and the polarization potential of Eq. (2.5), it was found that the cross section obtained by normalizing to the data in $2°<\theta<5°$ agree with the experimental values for $20°<\theta<40°$ within 2% or 3%, but in the angular range $5°<\theta<20°$ it only agrees within 5% to 10% in the energy range 200–700 eV. The partial wave analysis showed that the polarization potential has only negligible effects on the $d\sigma/d\omega$ for angles greater than 25°, while for smaller angles the two potentials contribute significantly. Since the form of the polarization potential is fixed, one needs to look into the modification of the static potential due to the interaction of the incident electron and the atomic electrons. The static potential in Eq. (2.9) is based on the Hartree–Fock ground state wavefunction of the unperturbed atom. To obtain a correction to this potential, consider the Hamiltonian of the two electron system (in atomic units)

$$H=-\frac{\nabla_1^2}{2}-\frac{\nabla_2^2}{2}-\frac{2}{r_1}-\frac{2}{r_2}+\frac{1}{|\mathbf{r}_1-\mathbf{r}_2|}. \quad (2.12)$$

The wavefunction in Eq. (2.8) is not an exact solution of the Schrödinger equation $H\Phi=E\Phi$ but instead a function that minimizes the expectation value of the Hamiltonian given by

$$E=\frac{\langle\Phi_0|H|\Phi_0\rangle}{\langle\Phi_0|\Phi_0\rangle}. \quad (2.13)$$

The wavefunction obtained by minimizing the expression in Eq. (2.13) using the orbital form of Eq. (2.8) represent a ground state with slightly larger energy of -2.86167 (a.u.) compared to the experimental value of -2.9037245. In the intermediate energy range, the incident electron interacts with the atom to change the ground state wavefunction only slightly, so that to obtain a correction to the interaction potential a reasonable approximation is to obtain a perturbed ground state wavefunction satisfying the equation

$$E=\frac{\langle\Phi|H|\Phi\rangle}{\langle\Phi|\Phi\rangle}=E_0+\Delta E, \quad (2.14)$$

where E_0 is the experimental value of the ground state energy and ΔE is a perturbation energy caused by the interaction treated phenomenologically. Once the wavefunction satisfying Eq. (2.14) is obtained, the correction to the static potential is then given by

$$\Delta V=\langle\Phi|V(\mathbf{r},\mathbf{r}_1,\mathbf{r}_2)|\Phi\rangle-\langle\Phi_0|V(\mathbf{r},\mathbf{r}_1,\mathbf{r}_2)|\Phi_0\rangle. \quad (2.15)$$

For a four-parameter orbital of the form

$$\phi_{1s}=(Ae^{-ar}+Be^{-br})(4\pi)^{-1/2} \quad (2.16)$$

the expectation value of the energy is calculated from the following:

$$\langle\Phi_0|\nabla_1^2|\Phi_0\rangle=\langle\Phi_0|\nabla_2^2|\Phi_0\rangle=-\frac{A^2}{4a}-\frac{B^2}{4b}-\frac{4abAB}{(a+b)^3},$$

$$\langle\Phi_0|\frac{1}{r_1}|\Phi_0\rangle=\langle\Phi_0|\frac{1}{r_2}|\Phi_0\rangle=\frac{A^2}{4a^2}+\frac{B^2}{4b^2}+\frac{2AB}{(a+b)^2},$$

$$\langle\Phi_0|\frac{1}{r_{12}}|\Phi_0\rangle=\frac{5}{128}(A^4a^{-5}+B^4b^{-5})+5A^2B^2(a+b)^{-5}$$
$$+\frac{A^2B^2}{8}\left[\frac{(a^2+b^2+3ab)}{(a+b)^3(ab)^2}\right]+\frac{2AB}{(a+b)^2}\left[\frac{A^2(11a^2+b^2+8ab)}{a^2(3a+b)^3}\right.$$
$$\left.+\frac{B^2(11b^2+a^2+8ab)}{b^2(3b+a)^3}\right]. \quad (2.17)$$

Using the same values for a and b as in the exponents in Eq. (2.8), one can vary the values of A and B within the condition

$$\langle\Phi_0|\Phi_0\rangle=\left\{\frac{A^2}{4a^3}+\frac{B^2}{4b^3}+\frac{4AB}{(a+b)^3}\right\}^2=1 \quad (2.17a)$$

to obtain various values of energy differing by a few percent from the Hartree–Fock ground state energy of -2.86168 (a.u.). For $A=2.5$, $B=2$ and $a=1.4$, $b=3$, the value of E using Eq. (2.17) is -2.8600075 (a.u.) with an average perturbation energy of 0.043717 (a.u.). Using the wavefunction corresponding to this energy, the correction term to the potential is found from Eq. (2.15) as

$$-\Delta V(r)=(0.377-0.11/r)e^{-2.8r}+(-0.23+0.27/r)e^{-6r}$$
$$+(-0.036-0.1/r)e^{-4.4r}. \quad (2.18)$$

It was found that this correction term depended on the energy of the incoming electron and also on the num-

ber of parameters and the form of the function used to represent the wavefunction. For the orbital of the form given by Eq. (2.8) an optimum correction term for which the computed cross section agreed with the experimental data at 500 eV was found to be (in units of Ry)

$$\Delta V(r) = -(0.106/r + 0.274 + 0.351r)\exp(-2.8r) + (0.087/r + 0.215 - 0.102r - 0.011r^2)\exp(-4.4r) + (0.019/r + 0.069 + 0.075r)\exp(-6r)\ . \quad (2.19)$$

The same correction term was used for all the calculations in the energy range 200–700 eV. However, no significant difference resulted in the cross sections when $\Delta V(r)$ above was approximated by

$$\Delta V(r) = -(0.25 + 0.31r)\exp(-2.8r)\ . \quad (2.20)$$

C. Correction for electron exchange scattering amplitude

For the range of energies and scattering angles considered here, a formula similar to the Born approximation is given by Bonham[22,23]

$$f^{ex}(\theta) = -(2N_{ex}k^{-2})\langle\Phi_0|\sum_j \exp(i\mathbf{K}\cdot\mathbf{r}_j)|\Phi_0\rangle\ , \quad (2.21)$$

where $K = 2k\sin(\theta/2)$ and the atomic scattering factor in Eq. (2.21) as computed by Brown[24] was used in the present calculations. For values of K in the range $0 < K < 2$, it was found that no significant change in the corrections would result if the atomic scattering factor is replaced by the approximation $F(K) = 2(1 + 0.204K^{2.127})^{-1}$ (error within ±0.5%).

III. NUMERICAL METHOD FOR THE SOLUTION OF THE SCATTERING EQUATIONS AND THE CALCULATION OF PHASE SHIFTS

A. Solution of the Schrödinger equation

The nonrelativistic quantum mechanical scattering model used in the present calculation is given by the Schrödinger equation

$$[\nabla^2 + k^2 - U(r)]\Psi(\mathbf{r}) = 0\ , \quad (3.1)$$

where ∇^2 is the Laplacian operator, $\mathbf{r}$ is the position vector of the scattered electron, and k is the wavenumber related to the energy by

$$k^2 = 2mE/\hbar^2\ ;\quad U(r) = (2m/\hbar^2)[\langle 0|V|0\rangle + V_p(r) + \Delta V(r)]\ . \quad (3.2)$$

Expansion of Eq. (3.1) in terms of partial waves, namely

$$\Psi(\mathbf{r}) = \sum_l A_l P_l(\cos\theta)\Psi_l(r)\ , \quad (3.3)$$

and using the orthonormality of $P_l(\cos\theta)$, one obtains a set of uncoupled differential equations given by

$$\frac{1}{r^2}\frac{d}{dr}\left(r^2\frac{d\Psi_l}{dr}\right) + \left[k^2 - U(r) - \frac{l(l+1)}{r^2}\right]\Psi_l(r) = 0\ , \quad (3.4)$$

where $l = 0, 1, \ldots$ correspond to the angular momentum associated with each partial wave. In the absence of the potential $U(r)$, the solution of Eq. (3.4) is that of the free wave, namely $\Psi_l \sim B_l kj_l(kr) + C_l kn_l(kr)$, where j_l and n_l are the spherical Bessel and Neuman functions, respectively; and for the scattering amplitudes, the solution of Eq. (3.4), which is bounded at the origin, must have the assymptotic form

$$\Psi_l \sim (1/kr)\sin[kr - (\pi l/2) + \delta_l(k)]\ , \quad (3.5)$$

where δ_l is the phase shift for the lth partial wave. Equation (3.4) was integrated outward using the following numerical procedure on an IBM 370–135 computer. In the numerical solution of the Schrödinger equation, the values of $\Psi_l(r)$ for small values of r in the range $0 < r < 0.1\ a_0$ were obtained from a power series expansion of the differential equation. Using these for initial values of $\Psi_l(r)$, a multistep algorithm was used for the numerical solution up to a maximum of $r = 50\ a_0$. The well-known Numerov[25] algorithm was used for all l values in the range $0 < l < 15$. For selected values of l the Adam–Moulton predictor corrector method was used for checking the solution obtained from the Numerov method. During the computation, it was found that for s waves ($l = 0$) the Adam–Moulton method gave more accurate values of the phase shifts compared to the Numerov method for the same length of computation while for larger values of l, the Numerov algorithm was found to be more efficient. For values of r in the range $0 < r < 0.2\ a_0$ a mesh size Δr of 0.001 to 0.005 a_0 was used for generating accurate values of Ψ_l needed for the multistep methods and a mesh size of 0.01–0.05 a_0 were used in testing the accuracy of the computed solutions for values of Ψ_l in the range $0 < l < 15$ and for energies in the range $100 < E < 700$ eV. It was found that for values of l greater than 12, some instability resulted near the origin for small values of the mesh size in the range 0.001–0.05 a_0. The Adam–Moulton method was found to be more stable in this respect. Near the origin, for large values of l, the function Ψ_l has a r^{l+1} behavior causing it to practically vanish and thus losing accuracy for the computed initial values. The overall accuracy of the numerical methods were tested using the well-known static potential of the electron–hydrogen problem given by $V(r) = -2(1 + 1/r)\times\exp(-2r)$. The phase shifts for this case agreed with those of Heaton and Moiseiwitsch[26] to four significant figures using Δr in the range 0.01–0.02 a_0. Another check on the accuracy of the solutions was done simply by comparing the solutions obtained when the outward integration was stopped at $r = 20\ a_0$ and turning the integration backwards to the origin. Comparison of the outward and inward solutions agreed to three of four significant figures for the intermediate energy range and for $l = 0$–12. After the program for the scattering cross section was completed, the dependence of the cross section values on the accuracy of the solution of Eq. (3.4) was also tested by computing the cross section with $\Delta r = 0.01$, 0.02, and 0.05 a_0 for an energy of 500 eV. It was found that a Δr of 0.05 a_0 produced significant changes in the cross section for scattering angles in the range $0° < \theta < 10°$, while for larger angles the change was found to be less pronounced. In all the calculations 0.02 a_0 was found to be sufficient for $l > 3$. At the energy of 500 eV used as a test case, a mesh size of 0.01 a_0 was used for all values of l up to 15.

TABLE I. Constancy of phase shifts evaluated at various roots of $\Psi_l(r)$ at 500 eV.

l	Roots (in a_0)	δ_l^{SCH}
1	15.232628	0.321454
	20.933514	0.321462
	24.561233	0.321464
2	15.511105	0.182964
	20.176284	0.182974
3	15.258500	0.1105696
	20.443396	0.110571
	24.590489	0.110574
4	15.157543	0.069519
	20.185563	0.069525
	24.852060	0.069521
5	15.253221	0.045186
	20.442198	0.045193
	24.591314	0.045195
10	15.448117	0.008848
	20.134683	0.008850
	24.812680	0.008850

Even though the accuracy of the phase shifts are found to depend on the value of Δr, the scattering cross section is found to be less sensitive on the accuracy of the phase shifts in the angular range $1° < \theta < 45°$. In the computation of the phase shifts, the roots of the function $\Psi_l(r)$ were used and the accuracy of this was checked by comparing the roots of $j_l(kr)$ at the energy of 500 eV for low values of l and with the potential function set equal to 0. It was found that somehow the roots were more accurate than the values of the function itself by one or two decimal places for various values of l.

B. Calculation of the phase shifts for $0 < l < 12$

Theoretically, the phase shifts are defined from the assymptotic condition that $r\Psi_l \sim \sin[kr - (\pi l/2) + \delta_l]$. This worked fine for s waves but was found to be impractical for $l > 0$. Outward integration in the range 100–500 a_0 showed a steady change in the value of the phase shifts obtained using the above condition. This is found to be due to the fact that the potential function drops off rapidly as r is increased beyond 50 a_0 while the term $l(l+1)/r^2$ still contributes to the solution. The standard procedure then is to compare the solution to the spherical Bessel and Neumann functions at a "matching radius." However, it was found that the phase shifts can be found with less computations if the roots of the functions Ψ_l are used instead of the values of the function. The equation used by Temkin and Lamkin[27] for the phase shift of the lth partial wave is given by

$$\delta_l(k) = \tan^{-1}[j_l(kr)/n_l(kr)] - N\pi + Q\pi + \tan^{-1}[s_l/(f_l - \Delta_l)] , \quad (3.6)$$

where the functions s_l, f_l, and Δ_l are given by[28]

$$f_l = rR_l'(r)/R_l(r) , \quad s_l = r(n_l j_l' - j_l n_l')(n_l^2 + j_l^2)^{-1} ,$$
$$\Delta_l = r(n_l' n_l + j_l' j_l)(n_l^2 + j_l^2)^{-1} ; \quad R_l = r\Psi_l . \quad (3.7)$$

Inspection of Eq. (3.7) shows that the last term in Eq. (3.6) vanish whenever $R_l(r) = 0$. Thus, if the root of R_l is used, in Eq. (3.6), it becomes

$$\delta_l = \tan^{-1}[j_l(kr_0)/n_l(kr_0)] - N\pi + Q\pi , \quad (3.8)$$

where N and Q are integers. In Eq. (3.8), the root r_0 can easily be calculated from the interpolation equation

$$r_0 \simeq r_{i+1} - (r_{i+1} - r_i)\{|R_l(r_{i+1})| + |R_l(r_i)|\}^{-1}|R_l(r_{i+1})| , \quad (3.9)$$

where r_i and r_{i+1} are such that the function R_l changes sign between them. For $\Delta r = 0.01$ a_0, the phase shifts computed from this procedure were found to be accurate to four or five significant figures. Table I shows the constancy of the phase shifts calculated with roots in the range $15 < r < 25$ a_0 for angular momentum in the range $0 < l < 10$ at 500 eV. Table II shows the constancy of the roots when the mesh size is changed from 0.01–0.02 a_0. Generally the roots are found to be accurate to five significant figures for $0 < l < 15$. Also, the phase shifts computed from the Born approximation are compared with those obtained from the above procedure at an energy of 500 eV. For all the calculations, the Born phase shifts were found to be sufficiently accurate for values of l greater than 12.

C. Phase shifts for $12 < l < 1000$

The phase shifts corresponding $l > 12$ were computed by a numerical evaluation of the integral in Eq. (3.10)

$$\delta_l(k) \simeq -k \int_0^\infty V_e(r)(\pi/2kr)[J_{l+1/2}(kr)]^2 r^2 dr . \quad (3.10)$$

A nine point quadrature formula was used for values of l up to 30 for all energies and, for $l > 30$, an approximate expression in terms of the Gamma function is derived. The algorithm for the numerical integration of Eq. (3.10) is given by the following:

TABLE II. Comparison of the Schrödinger and Born phase shifts (500 eV).

l	Mesh size Δr (in a_0)	Schrödinger phase shifts (radians)	Born phase shifts (radians)
0	0.02	0.644033	0.610936
	0.01	0.645168	
1	0.02	0.321645	0.305113
	0.01	0.321465	
2	0.02	0.182984	0.176160
	0.01	0.182969	
3	0.02	0.110629	0.107689
	0.01	0.110566	
4	0.02	0.069576	0.068282
	0.01	0.069516	
5	0.02	0.045226	0.044655
	0.01	0.045196	
6	0.02	0.030374	0.030120
	0.01	0.030354	
10	0.02	0.008898	0.008839
	0.01	0.008844	

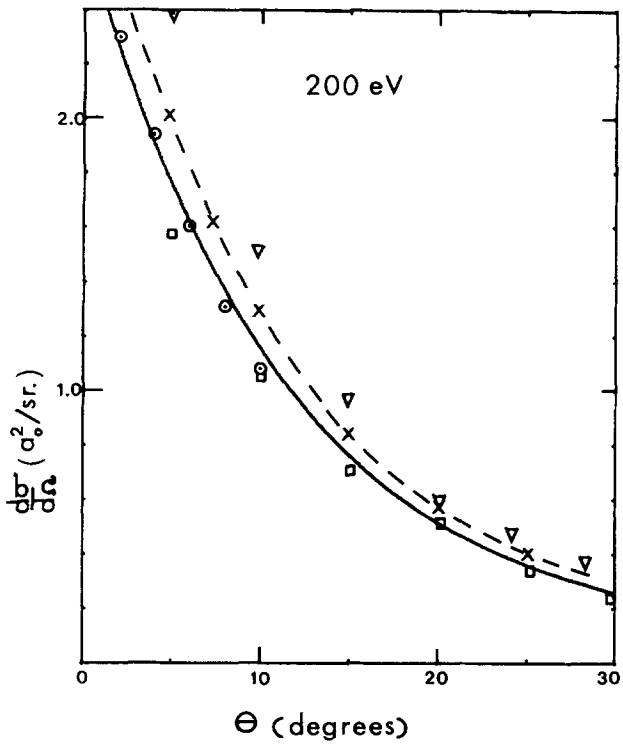

FIG. 1. Comparison of the differential scattering cross section with the experimental data at an incident energy of 200 eV. Solid line is the $d\sigma/d\Omega$ with $C=12.25$, dashed line repersents the $d\sigma/d\Omega$ of eikonal theory (Ref. 34). Circles are the data of Bromberg (Ref. 14) and the triangles, squares, and crosses represent other experimental data as reported in Ref. 34.

$$\delta_l \simeq -k \sum_{\mu=1}^{N} \sum_{\nu=1}^{N} A_\nu V_e(\chi_{\mu\nu}) j_l^2(k\chi_{\mu\nu}) \chi_{\mu\nu}^2 \frac{(r_2-r_1)}{M} \quad , \quad N=9 \, , \tag{3.11}$$

where

$$\chi_{\mu\nu} = (r_2-r_1)[(\mu-1)+(\nu-1)/(N-1)]M^{-1}$$

and the constants A_ν are $A_1 = A_9 = 0.034885361552028$, $A_2 = A_8 = 0.20768959435$, $A_3 = A_7 = -0.0327336866067$, $4_4 = A_6 = 0.37022927689$, and $A_5 = -0.160141093474427$. For the efficient evaluation of the integral, it was found that range of integration $(0, \infty)$ should be truncated to (r_1, r_2) in which r_1 varies from $0.01-5\ a_0$ for l in the range from 1–40 and r_2 is changed from 50–100 a_0. The value of the integer M in Eq. (3.12) controls the subdivision of the interval (r_1, r_2). For the intermediate energy range, this was varied from 50 to 100. The numerical integration program was tested with certain functions for the potential for which the partial wave integral can be evaluated in terms of known functions. It was found that for the scattering cross sections in the angular range $1° < \theta < 20°$, 100 to 200 partial waves are required. The algorithm of Eq. (3.11) was found to be slow when such large numbers of partial waves are required. For phase shifts in the energy range $100 < E < 700$ eV and $l > 30$, an approximation is derived on the basis that most of the contribution to the integral in Eq. (3.10) comes from larger values of r. To see this,

TABLE III. Comparison of phase shifts calculated analytically and by numerical integration for large values of l.

l	(numerical) δ_l^{Born} (in radians)	(analytical) δ_l^{Born} (in radians)
21	0.001709	0.001691
22	0.001525	0.001504
23	0.001364	0.001353
24	0.001223	0.001217
25	0.001100	0.001097
26	0.000992	0.000990
27	0.000897	0.000896
28	0.000812	0.000813
29	0.000738	0.000739
30	0.000672	0.000673
40	0.000297	0.000297
50		0.000155
100		0.00001975
200		0.00000252

consider Gegenbauer's generalization of the spherical Bessel function given by

$$j_l(Z) = \frac{Z^l}{2^{l+1}l!} \int_0^\pi \cos(Z\cos\theta) \sin^{2l+1}\theta d\theta \, . \tag{3.12}$$

Writing the integral of Eq. (3.10) in two parts, one finds that for $l > 30$, $kr_1 < 10$

$$\int_0^{r_1} V_e(r) j_l^2(kr) r^2 dr < 10^{-25} \int_0^{r_1} V_e(r) r^2 dr \simeq 0 \, . \tag{3.13}$$

Thus, within the degree of accuracy required in the calculations, the integral can be approximated by

$$\delta_l(k) \simeq -k \int_{r_1}^{\infty} [\langle 0|V|0\rangle + \Delta V + V_p(r)] j_l^2(kr) r^2 dr \, , \tag{3.14}$$

where for $l > 30$, r_1 can be chosen to be between 1 and 10 a_0 in the energy range 100–700 eV. In the numerical evaluation of this integral with the potential defined by Eq. (2.9), it is found that most of the contribution to this integral comes from the second part of the integrand and this can be expanded in ascending powers of (C/r) to obtain the following expression for the integral in terms of Gamma functions:

TABLE IV. Differential scattering cross section (in a_0^2/ sr) using various numbers of partial waves for 500 eV.

θ (degrees)	$N=20$	$N=40$	$N=60$	$N=100$	$N=150$	$N=200$
2	1.159	1.393	1.441	1.436	1.414	1.415
4	1.051	1.121	1.086	1.076	1.084	1.082
6	0.899	0.854	0.842	0.853	0.850	0.849
10	0.584	0.552	0.555	0.556	0.555	0.555
20	0.215	0.218	0.218	0.218	0.218	0.218
30	0.091	0.091	0.091	0.091	0.091	0.091
40	0.040	0.040	0.040	0.040	0.040	0.040

$$\delta_l(k) \cong -k \int_{r_1}^{\infty} [\langle 0|V|0\rangle + \Delta V] j_l^2 r^2 dr + \frac{\pi \alpha_4}{4C^2} \sum_{\mu=1}^{N} \left[\frac{(-C)^{\mu+1} \left(\frac{k}{2}\right)^{4\mu-2} \Gamma(4\mu-1)\Gamma(l-2\mu+\frac{3}{2})}{\Gamma(2\mu)\Gamma(2\mu)\Gamma(l+2\mu+\frac{1}{2})} \right]$$

where

$$\frac{C^{1/4}k}{l} < 1/2\,, \quad l > 30, \quad N = [(2l+3)/4]\,. \tag{3.15}$$

Table III shows the comparison between the exact numerical integration of Eq. (3.10) and the values obtained from Eq. (3.15) at the energy of 500 eV and for $C = 52.7$ for values of $l > 20$. The differential scattering cross section is calculated from the scattering amplitude given by[29]

$$f(\theta) = (2ik)^{-1} \sum_{l=0}^{N} (2l+1)[\exp(2i\delta_l) - 1] P_l(\cos\theta)\,,$$

where $P_l(\cos\theta)$ are the Legendre polynomials generated using their recursion relation.[30] The effect of using a finite number of terms is shown in Table IV. It is seen from this that at angles in the range $2° < \theta < 6°$ about 200 partial waves are required to determine the cross section within 1% at the energy of 500 eV. For scattering angles less than 1°, it was found that more than 1000 partial waves are required.

IV. DISCUSSION OF RESULTS AND COMPARISON WITH OTHER CALCULATIONS

Comparison of the calculated differential scattering cross sections $d\sigma/d\Omega$ with the experimental data of Bromberg[14] and others[31–33] are shown in Figs. 1–5. For the determination of the energy-dependent parameter in the potential $V_p(r)$, the data of Bromberg at $\theta = 2°$ was used since this was the most recent and comprehensive data available. The agreement between the calculated $d\sigma/d\Omega$ and the data of Bromberg is satisfactory at all energies and angles while, as shown in Figs. 1, 3, and 4, they differ somewhat from other experimental data at smaller scattering angles. For scattering angles $\theta > 20°$, the cross sections agree well with the experimental data. The agreement is also satisfactory with the data of Vriens, Kuyatt, Mielczarek, and Chamberlain[31,32] for the angular range shown.

The energy dependent parameters C and δ defining the potential $V_p(r)$ were found to have a noticeable effect (1%–5%) on the computed partial wave phase shifts. However, it was found that the cross sections were somewhat insensitive to the variation of δ and so a fixed value of δ was used for all energies and C was varied for each energy to obtain normalization at $\theta = 2°$ within 1%–3% for 300–700 eV. The values of the parameter were then found to be given by the approximation $C = (1.3 + E/350)^4$ for $\delta = 8$, where E is the incident electron energy in eV. The values of C obtained from this equation were then used for the calculation of $d\sigma/d\Omega$ and forward scattering amplitudes for all other energies

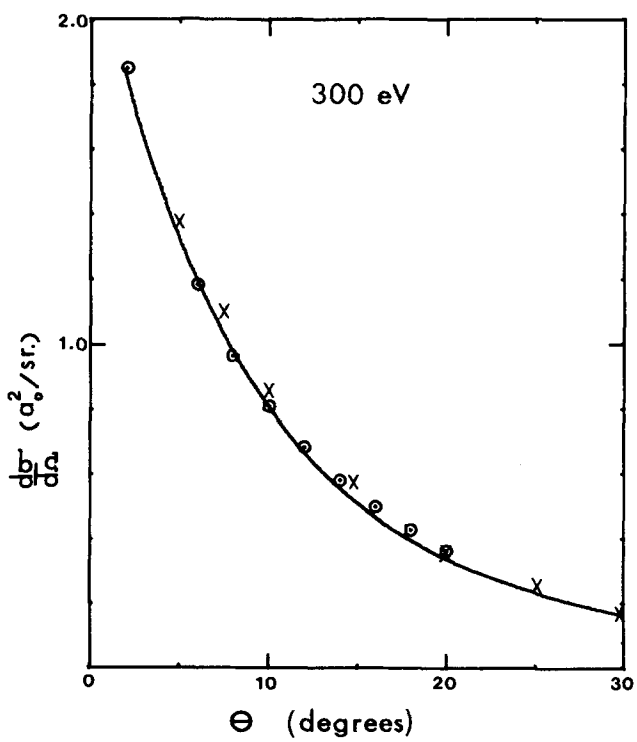

FIG. 2. Comparison of the $d\sigma/d\Omega$ with the experimental data at an incident electron energy of 300 eV. The solid line and circles denote the same as in Fig. 1 and crosses represent the data of Vriens *et al.* (Ref. 31).

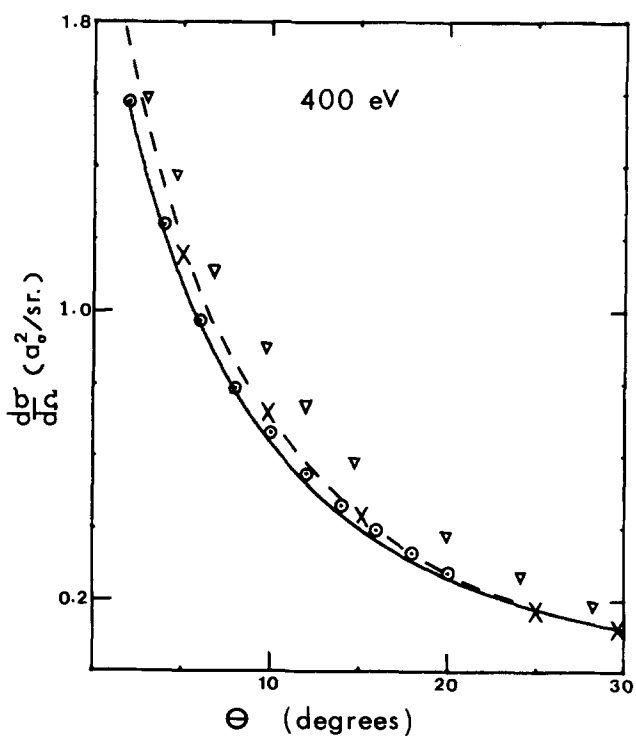

FIG. 3. Comparison of $d\sigma/d\Omega$ with the experimental data at an incident electron energy of 400 eV, with $C = 21.37$. All the symbols are the same as in Fig. 1.

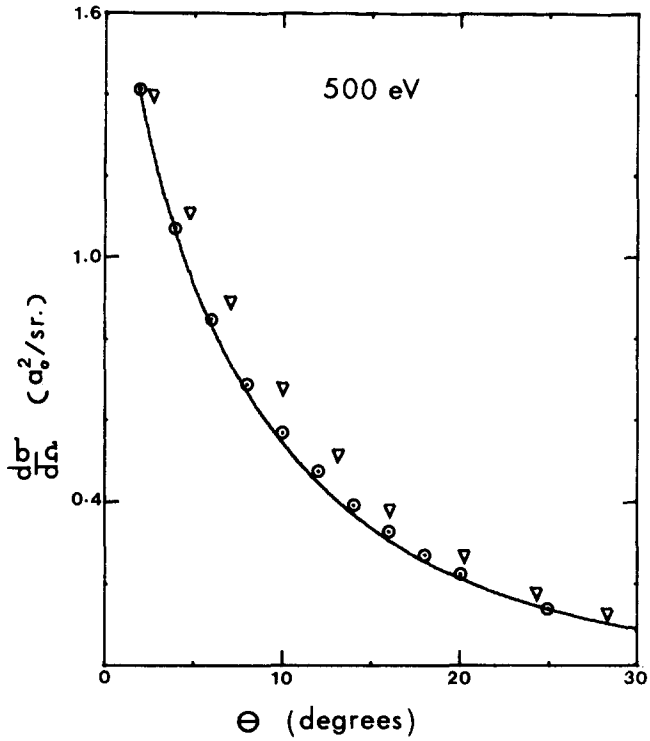

FIG. 4. Comparison of $d\sigma/d\Omega$ with the experimental data at an incident electron energy of 500 eV. $C = 53.14$. All symbols represent the same data as in Fig. 1.

in the range $100 < E < 1000$ eV in steps of 100 eV. The partial wave phase shifts obtained from this model are compared with the results of Ganas, Dutta, and Green[12] and LaBahn and Callaway[9] as shown in Table V and, the

TABLE V. Comparison of phase shifts with the results (500 eV) of (a) LaBahn and Callaway and (b) Ganas, Duttan, and Green.

l	(a) δ_l(radians)	(b) δ_l(radians)	Present calculation δ_l(radians)
0	0.6417	0.6429	0.6452
1	0.3121	0.3194	0.3215
2	0.1751	0.1811	0.1830
3	0.1086	0.1094	0.1106
4	0.0729	0.0689	0.0695
5	0.0518	0.0450	0.0452
6	0.0382	0.0305	0.0304
7	0.0289	0.0214	0.0210
8	0.0222	0.0156	0.0152
9	0.0172	0.0117	0.0114
10	0.0126	0.0091	0.0089

calculated values of $d\sigma/d\Omega$ are compared with the data of Bromberg in Table VI for an energy of 500 eV. It can be seen in Table VI that the inclusion of the correction term $\Delta V(r)$ improves the agreement with the experimental data in the angular range $5° < \theta < 20°$. An approximate form of the correction term using the function $(C_1 + rC_2)\exp(-2.8r)$ was tested in the computation of $d\sigma/d\Omega$ and it was found that C_1 and C_2 lie in the ranges (0.2, 0.4) and (0.3, 0.7), respectively, for which the computed $d\sigma/d\Omega$ were in fairly good agreement with the experimental data. For a given pair of

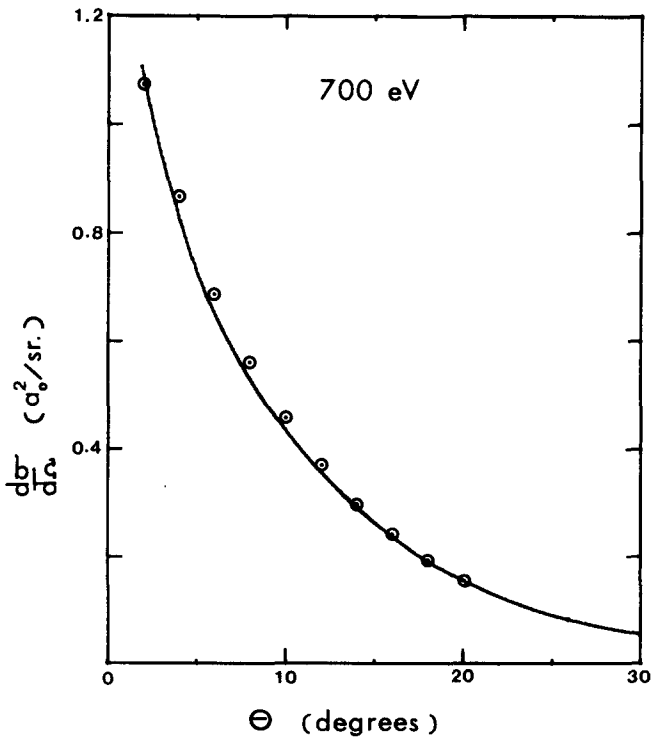

FIG. 5. Comparison of $d\sigma/d\Omega$ with the experimental data at an incident electron energy of 700 eV. Solid line represents calculated $d\sigma/d\Omega$ with $C = 118.59$ and circles represent the data of Bromberg (Ref. 14).

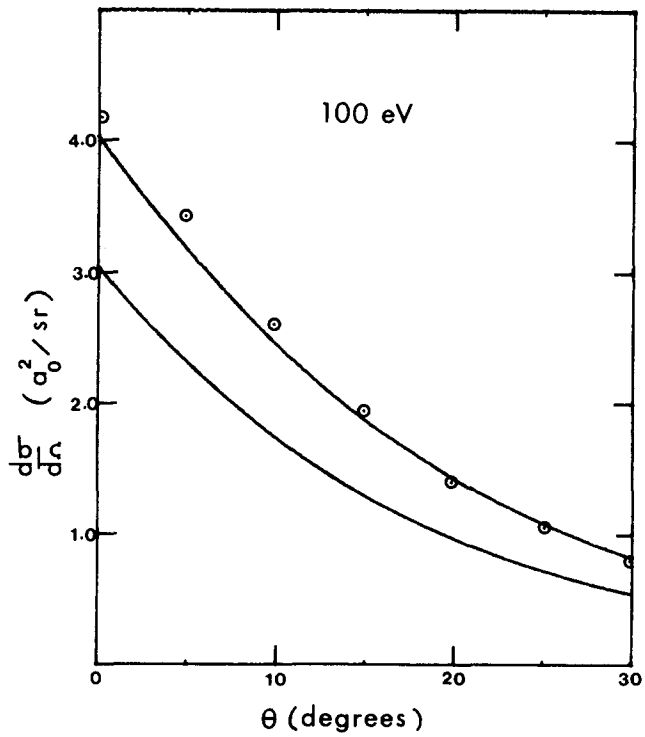

FIG. 6. Comparison of the differential scattering cross section $d\sigma/d\Omega$ obtained from the present model (with the correction for electron exchange scattering) with the results of Byron *et al.* Upper curve represents $d\sigma/d\Omega$ with allowance for electron exchange scattering at 100 eV and the lower curve is the $d\sigma/d\Omega$ without this correction. Circles represent the values of $d\sigma/d\Omega$ obtained by the optical eikonal theory (Ref. 34).

TABLE VI. Comparison of calculated values of cross section (in a_0^2/sr) with the experimental data of Bromberg at 500 eV. (a) Calculated $d\sigma/d\Omega$ without the correction term $\Delta V(r)$, with $C = 2.5^4$ and (b) $d\sigma/d\Omega$ with ΔV included with $C = 2.7^4$.

Angle θ (degrees)	$\frac{d\sigma}{d\Omega}$ [a] (a_0^2/sr)	$\frac{d\sigma}{d\Omega}$ [b] (a_0^2/sr)	$\frac{d\sigma}{d\Omega}$ (exptl) (a_0^2/sr)
2	1.400	1.413	1.413
4	1.054	1.081	1.072
6	0.818	0.849	0.848
8	0.647	0.682	0.689
10	0.520	0.555	0.570
12	0.423	0.456	0.476
14	0.348	0.377	0.394
16	0.288	0.313	0.330
18	0.240	0.260	0.273
20	0.202	0.218	0.226
30	0.088	0.091	0.089
40	0.040	0.040	0.041

C_1 and C_2, the energy dependent parameter C had to be changed to have the normalization of $d\sigma/d\Omega$ at $\theta = 2°$. Nonzero values of C_1 and C_2 were found to affect the agreement with the experimental data at larger angles thus indicating that the improvement in the angular range $5° < \theta < 20°$ is not entirely consistent with theoretical predictions at large angles of scattering. This is an indication that the potential is not general enough to accurately account for the experimental data in the above angular range in which a larger contribution from open inelastic channels might be expected to be significant. The normalization at the small angle region partially allows for the inelastic effects in a phenomenological way by the polarization potential $V_p(r)$ which does not affect the $d\sigma/d\Omega$ at large angles because of its long range behavior. However, the variation of the parameters in $V_p(r)$ did not seem to improve the results any further in the above angular range and thus it seems that, to obtain better agreement with the experimental data, one has to use an imaginary part in the effective potential to account for the open inelastic channels that contribute to the scattering cross sections. The added correction term $\Delta V(r)$ might be given the interpretation that the incident electron "sees" an average distorted static field of the target atom which is slightly different from $\langle \Phi_0 | V | \Phi_0 \rangle$ as a result of the interaction at short distances from the atom while this

TABLE VII. Comparison of the total cross sections (in units of a_0^2) for the elastic scattering of electrons by helium obtained by (a) present model, (b) Ganas, Dutta, and Green (Ref. 12), and (c) LaBahn and Callaway (Refs. 8 and 9).

E (eV)	σ^a	σ^b (in units of a_0^2)	σ^c
100	2.125	2.264	2.230
200	0.970	0.995	0.977
300	0.609	0.608	0.609
400	0.440	0.430	0.441
500	0.343	0.331	
1000	0.164		

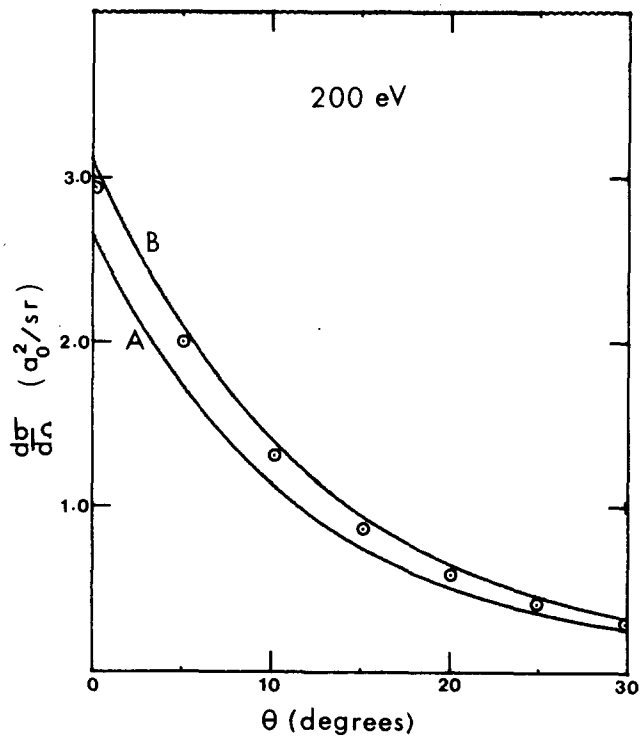

FIG. 7. Same as in Fig. 6 but at a different incident electron energy of 200 eV.

picture does not seem to be very accurate for partial waves of low angular momentum ($0 \leq l < 10$), which determine most of the contribution to $d\sigma/d\Omega$ for large angles. On the other hand, the inclusion of the polarization potential $V_p(r)$ had less effect on $d\sigma/d\Omega$ at large angles and this made it possible to obtain an optimum value of the parameter mostly by requiring the normalization condition at small angle for a given energy. Table IV illustrates this fact to some extent. It is seen that inclusion of partial waves of $l > 20$ changes the values of $d\sigma/d\Omega$ significantly at smaller angles, and it may be recalled that contribution to δ_l for $l > 20$ comes from the polarization potential. A comparison of the total cross section with the results of Ganas *et al.* and LaBahn and Callaway is shown in Table VII. It is seen that the present results are in very good agreement with their results.

TABLE VIII. Comparison of the differential scattering cross section $d\sigma/d\Omega$ calculated using (a) present model with electron exchange correction and (b) optical eikonal model of Byron and Joachain (Ref. 34) at incident electron energies 200 and 400 eV (in a_0^2/sr).

θ (deg)	$d\sigma/d\Omega^a$ ($E = 200$ eV)	$d\sigma/d\Omega^b$ ($E = 200$ eV)	$d\sigma/d\Omega^a$ ($E = 400$ eV)	$d\sigma/d\Omega^b$ ($E = 400$ eV)
0	3.11	2.97	2.16	2.15
5	2.11	2.03	1.13	1.14
10	1.41	1.28	0.64	0.675
15	0.95	0.85	0.405	0.435
20	0.65	0.58	0.27	0.28
25	0.46	0.41	0.18	0.18
30	0.33	0.29	0.12	0.12

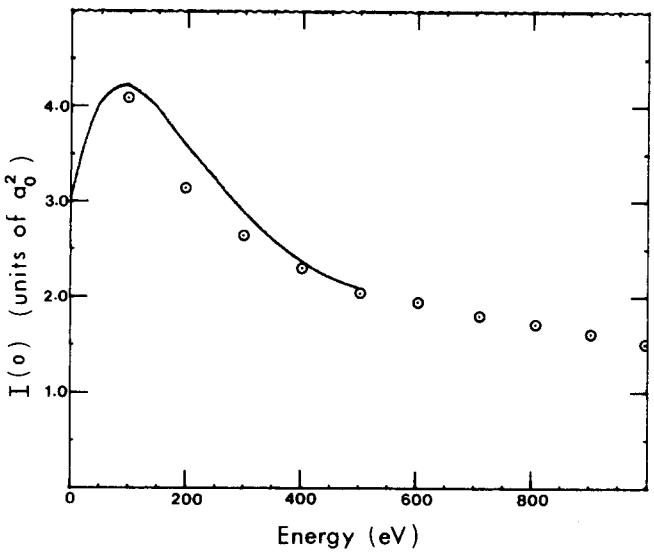

FIG. 8. Comparison of the forward scattering intensity $I(0)$ (in a.u.) predicted by the present model and the results of dispersion relations of Bransden and McDowell (Ref. 35). Solid line ($E < 500$ eV) represents the theoretical data of Ref. 35 and circles represent the calculated values of $I(0)$ using 2 000–10 000 partial wave phase shifts including the correction for electron exchange scattering amplitude in the present model.

A comparison of the calculated $d\sigma/d\Omega$ at 100, 200, and 400 eV with the results of the optical eikonal theory of Byron and Joachain[34] is also shown in Figs. 1, 3, and 4. The comparison for 500 eV is not shown since the two $d\sigma/d\Omega$ lines overlapped. At lower incident energies there is less agreement and this is shown to be due to the effect of electron exchange scattering as shown in Figs. 6 and 7. When the correction for electron exchange is included in the calculation of $d\sigma/d\Omega$, the present results agree quite well with the predictions of optical eikonal theory. Table VIII shows the comparison of the numerical results with the inclusion of the correction at 400 and 200 eV. It was found that at higher energies the agreement improved.

Finally, the forward scattering amplitudes and intensities predicted by the present model for various energies are compared with the results of dispersion relations of Bransden and McDowell.[35] For the forward scattering amplitudes, a large number of partial waves were needed for convergence to within an uncertainty of 1% for energies in the range 100–1000 eV in steps of 100 eV. To obtain the forward scattered intensity $I(0)$ in the 500–1000 eV range, up to 10 000 partial wave phase shifts were used. The values obtained for $I(0)$ using the present model along with the plot of $I(0)$ of Bransden *et al.* are presented in Fig. 8. When corrected for electron exchange amplitude, the forward scattered intensities predicted by the present model are in good agreement with the results obtained by dispersion relations except at lower energies ($E < 300$ eV). The deviations at lower energies might be interpreted as due to the limitations of the present effective potential and partly due to the uncertainties of the experimental data at small angles. The agreement with the results of dispersion relations seem to improve steadily with the incident electron energy as seen from Fig. 8 and, at 1000 eV, the present model predicts a value of 1.50 (a.u.) compared to the 1.56 of dispersion theory. Tables IX and X show a comparison of the real part of the scattering amplitudes Re$f(0)$ (in a.u.) with

TABLE IX. Comparison of the real part of the forward scattering amplitude Re$f(0)$ calculated from the model potential and the results obtained by (a) optical eikonal model (Ref. 34) and (b) dispersion relations (Ref. 35).

E (eV)	Re$f(0)$ (in a.u.)	Re$f(0)^b$	Re$f(0)^a$
100	1.967	1.905	1.68
200	1.743	1.706	1.44
300	1.605	1.482	1.32
400	1.508	1.360	1.25
500	1.433	1.286	1.21
1000	1.220	1.117	

TABLE X. Comparison of the forward scattered intensity $I(0)$ (in a.u.) calculated from the present model with exchange scattering and the results obtained from (a) optical eikonal model (Ref. 34) and (b) dispersion relations (Ref. 35) for various incident electron energies E (in eV).

E	$I(0)$	$I(0)^a$	$I(0)^b$
100	4.08	4.20	4.20
200	3.00	3.13	3.59
300	2.63		2.86
400	2.31	2.15	2.41
500	2.08	1.97	2.14
1000	1.50		1.56

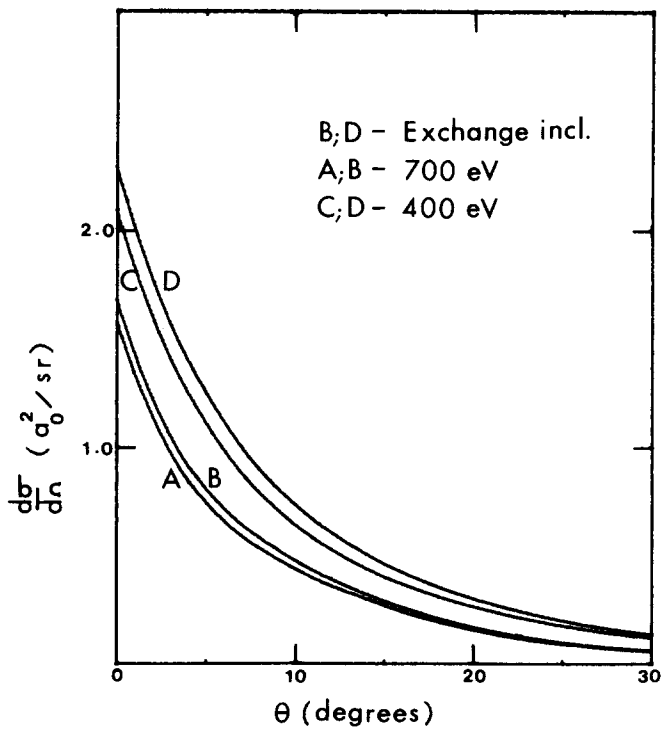

FIG. 9. Comparison of the effect of electron exchange scattering on the calculated $d\sigma/d\Omega$ at incident electron energies 400 and 700 eV as a function of the scattering angle θ.

the results of dispersion relations and optical eikonal theories. At all energies, Re$f(0)$ seem to differ somewhat with the results of dispersion relations. This might be partly due to the inadequacy of the first order exchange amplitude corrections which suffer from the same limitations as the Born approximations at low incident energies of the electron. The effect of the correction for electron exchange scattering is shown to decrease with the incident energy of the electron in Fig. 9. For energies > 300 eV, the effect of this correction on $d\sigma/d\Omega$ seems to lie well within the deviations of the cross section data as reported by various labs. Since the nonlocality in the effective potential is a result of the electron exchange contribution to the elastic scattering,[36] it appears that, in the energy range in which exchange scattering amplitude can be adequately represented by the first order approximation, the lack of nonlocality of the effective interaction potential is not a serious limitation of the model for the qualitative description of the scattering cross section. This might partly explain the good agreement of the present results with other theoretical and experimental data in the intermediate energy range. However, it is felt that to accurately account for the effects of open inelastic channels, a complex effective potential is needed to represent the interaction for lower incident electron energies; this work is in progress.

ACKNOWLEDGMENTS

The author wishes to thank Drs. H. D. Rutledge and D. H. Froemsdorf for providing the remote terminals for IBM 360 and 370 computing facilities used in the present calculations. A research grant awarded by the Grants and Research Funding Committee of Southeast Missouri State University is also acknowledged.

[1]P. G. Burke, A. Hibbert, and W. D. Robb, J. Phys. B **4**, 153 (1971); S. P. Khare and B. L. Moiseiwitsch, Proc. Phys Soc. London **85**, 821 (1965); L. Yriens, C. E. Kuyatt, and S. R. Mielczarek, Phys. Rev. **170**, 163 (1968); S. P. Khare and B. L. Moiseiwitsch, J. Phys. B **4**, 208 (1971); E. N. Lassettre, A. Skerbele, and M. A. Dillon, J. Chem. Phys. **49**, 2382 (1968); N. R. Kestner, J. Jortner, M. H. Cohen, and S. A. Rice, Phys. Rev. Sect. A **140**, 56 (1965); P. M. Morse and W. P. Allis, Phys. Rev. **44**, 269 (1933).
[2]K. Smith, *The Calculation of Atomic Collision Processes* (Wiley-Interscience, New York, 1971).
[3]H. S. W. Massey and Moussa, Proc. Phys. Soc. London **71**, 38 (1958).
[4]A. Temkin and J. C. Lamkin, Phys. Rev. **121**, 788 (1961).
[5]K. Smith and P. G. Burke, Phys. Rev. **123**, 174 (1961).
[6]P. G. Burke, Phys. Rev. **126**, 147 (1962).
[7]A. Temkin and J. C. Lamkin, Phys. Rev. **107**, 1004 (1957).
[8]J. Callaway and R. W. LaBahn, Phys. Rev. **168**, 12 (1968).
[9]R. W. LaBahn and J. Callaway, Phys. Rev. **180**, 91 (1969).
[10]M. H. Mittleman, Phys. Rev. A **2**, 1846 (1970).
[11]M. H. Mittleman and K. M. Watson, Phys. Rev. **113**, 198 (1959).
[12]J. E. Purcell, R. A. Berg, and A. E. S. Green, Phys. Rev. A **2**, 107 (1970); P. S. Ganas, S. K. Dutta, and A. E. S. Green, *ibid.* **2**, 111 (1970).
[13]J. P. Bromberg, J. Chem. Phys. **50**, 3906 (1969).
[14]J. P. Bromberg, J. Chem. Phys. **61**, 963 (1974).
[15]C. C. J. Roothan, Rev. Mod. Phys. **32**, 179 (1960).
[16]R. A. Buckingham, Proc. R. Soc. London Ser. A **160**, 94 (1937).
[17]H. A. Bethe, Handb. Phys. **24**, 339 (1943).
[18]M. L. Goldberger and K. M. Watson, *Collision Theory* (Wiley, New York, 1964), Chap. 11, p. 851; C. J. Joachain and M. H. Mittleman, Phys. Rev. A **4**, 1492 (1971).
[19]N. F. Mott and H. S. W. Massey, *The Theory of Atomic Collisions* (Oxford University, New York, 1965), p. 89.
[20]C. C. J. Roothan, L. M. Sachs, and A. W. Weiss, Rev. Mod. Phys. **32**, 186 (1960).
[21]L. B. Mendelsohn, F. Biggs, and J. B. Mann, Phys. Rev. A **2**, 1130 (1970).
[22]R. A. Bonham, J. Chem. Phys. **36**, 3260 (1962).
[23]R. A. Bonham, Phys. Rev. A **3**, 298 (1971).
[24]R. T. Brown, Phys. Rev. A **1**, 1342 (1970).
[25]A. C. Allison, J. Comput. Phys. **6**, 378 (1970); J. W. Cooley, Math. Comput. **15**, 363 (1961); D. R. Hartree, *The Calculation of Atomic Structure* (Wiley, New York, 1957).
[26]M. Heuton and B. L. Moiseiwitsch, J. Phys. B **4**, 338 (1971).
[27]Equation (3.4) of Ref. 4.
[28]J. B. Blatt and V. F. Weisskopf, *Theoretical Nuclear Physics* (Wiley, New York, 1952), p. 332.
[29]Page 567 of Ref. 19.
[30]M. Abramowitz and I. A. Stegum, *Handbook of Mathematical Functions* (U. S. Dept. of Commerce, Washington, DC, 1964).
[31]L. Vriens, C. E. Kuyatt, and S. R. Mielczarek, Phys. Rev. **170**, 163 (1968).
[32]G. E. Chamberlain, S. R. Mielczarek, and C. E. Kuyatt, Phys. Rev. A **2**, 1905 (1970).
[33]Experimental data of electron–helium scattering cross section as quoted in Ref. 34.
[34]F. W. Byron, Jr. and C. J. Joachain, Phys. Rev. A **9**, 2559 (1973).
[35]B. H. Bransden and M. R. C. McDowell, J. Phys. B **3**, 29 (1970).
[36]R. E. Schenter and R. M. Thaler, Phys. Rev. **146**, 70 (1966).